Journal of Solid Mechanics and Materials Engineering

Vol. 4, No. 7, 2010

Coupled Analysis of Hydrogen Transport using ABAQUS*

Chang-Sik OH**, Yun-Jae KIM** and Kee-Bong YOON***

** Department of Mechanical Engineering, Korea University

1 Anam-Dong, Sungbuk-ku, Seoul, Korea

E-mail:kimy0308@korea.ac.kr

*** Depatment of mechanical Engineering, Chungang University

Huksuk-Dong, Dongjak-ku, Seoul, Korea

Abstract

This paper describes two user subroutines developed within ABAQUS to simulate coupled hydrogen transport equations. Developed user subroutines incorporate two key features in coupled hydrogen transport equations, such as the hydrostatic stress and plastic strain effects on hydrogen transport, and hydrogen-induced dilatational deformation rate. To validate developed subroutines, present simulation results are compared with published results, showing good agreements for all cases considered.

Key words: ABAQUS, Hydrogen Transport Simulation

1. Introduction

Hydrogen embrittlement is a severe environmental type of failure[1-3]. Full-scale tests under high pressure and temperature conditions with hydrogen environments can be not only very expensive but also dangerous, which makes extensive tests difficult. In this respect, a numerical simulation technique would be needed as a complementary approach, based on which hydrogen-related failure can be simulated. Although extremely useful, such a simulation requires all the necessary constitutive equations related to hydrogen-related failure. Although mechanisms responsible for hydrogen-related failure are still in debate, an important aspect of hydrogen embrittlement is that there exists a transport stage of hydrogen to the sites where degradation occurs. Thus the analysis of the hydrogen transport processes should precede any attempt to address the issue of hydrogen embrittlement and hydrogen-related failure. Constitutive equations relevant to hydrogen transport processes are well summarized in Refs. (3) and (4). One notable point is that important variables affecting hydrogen transport include the hydrostatic stress and plastic strain, and thus hydrogen transport equations are fully coupled with elastic-plastic deformation. The research group at University of Illinois implemented coupled hydrogen transport equations and published a number of papers related to hydrogen transport and embrittlement[2-8]. The developed code, however, is based on an in-house code, not on general purpose finite element (FE) programs. Considering possible needs of numerical simulations of hydrogen-related failure in the near future, implementation of hydrogen transport equations into general purpose FE programs would be desirable.

This technical note explains implementation of hydrogen transport equations into the general purpose FE program, ABAQUS[9]. To incorporate effects of the hydrostatic stress

*Received 16 Nov., 2009 (No. t2)
[DOI: 10.1299/jmmp.4.908]

and plastic strain on hydrogen transport, two user subroutines are developed. To validate the developed subroutines, present results are compared with published ones in Ref. (4).

Nomenclature

θ_L : occupancy of the NILS
θ_T : occupancy of the trapping sites
W_B : trap binding energy
R : gas constant (=8.31J/mol/K)
T : absolute temperature (K)
C_T : hydrogen concentration per unit volume in trapping sites
C_L : hydrogen concentration in NILS
N_T : trap density measured in number of traps per unit volume
N_L : number of solvent lattice atoms per unit lattice volume
α : number of sites per trap
β : number of NILS per solvent atom
N_A : Avogadro's number ($6.0232\text{x}10^{23}$)
V_M : molar volume of the host lattice measured in units of volume per lattice mole
D_L : hydrogen diffusion constant through NILS
D_{eff} : effective diffusion constant
V_H : partial molar volume of hydrogen in solid solution

Abbreviation

NILS Normal interstitial lattice site

2. Hydrogen Diffusion Model

2.1 Hydrogen Transport Model in an Elastic-Plastic Solid

Assume that hydrogen diffusion occurs by normal interstitial lattice site (NILS) diffusion and that transported hydrogen resides either at NILS or at trapping sites. Relevant constitutive equations and detailed explanations are given in Ref. (4), and only the final equations are summarised here. The governing equation for transient hydrogen diffusion accounting for trapping and hydrostatic drift are given by

$$\frac{D_L}{D_{eff}}\frac{\partial C_L}{\partial t} - D_L\nabla^2 C_L + \nabla\cdot\left(\frac{D_L C_L V_H}{3RT}\nabla\sigma_{kk}\right) + \alpha\theta_T\frac{dN_T}{d\varepsilon_p}\frac{\partial\varepsilon_p}{\partial t} = 0$$
$$D_{eff} = \frac{D_L}{\left[\dfrac{C_L + C_T(1-\theta_T)}{C_L}\right]} \quad (1)$$

where $\partial/\partial t$ is the time derivative. In Eq. (1), D_L is the hydrogen diffusion constant through NILS; D_{eff} is an effective diffusion constant that varies pointwise; C_T is the hydrogen concentration per unit volume in trapping sites; C_L is the hydrogen concentration per unit volume in normal interstitial lattice sites (NILS); θ_T denotes the occupancy of the trapping sites; N_T denotes the trap density which is a function of the local effective plastic strain ε_p, i.e., $N_T = N_T(\varepsilon_p)$, and is measured in number of traps per unit volume; α denotes the number of sites per trap; V_H is the partial molar volume of hydrogen in solid solution; σ_{ij} is the Cauthy stress; R is the gas constant (R=8.31 J/(moleK); and T is the absolute temperature.

As hydrogen is assumed to reside either at normal interstitial lattice sites (NILS) or reversible trapping sites generated by plastic deformation. The two populations according to Oriani's theory[10] are always in equilibrium, and the occupancy θ_L of NILS sites is related to the occupancy θ_T of the trapping sites through the trap binding energy W_B:

$$\frac{1-\theta_T}{\theta_T}=\frac{1-\theta_L}{\theta_L}\exp\left(\frac{W_B}{RT}\right) \tag{2}$$

In addition, relationships

$$C_L=\theta_L\beta N_L \quad ; \quad C_T=\theta_T\alpha N_T \tag{3}$$

hold for the concentrations in NILS and trapping sites, respectively, where β denotes the number of NILS per solvent atoms; $N_L=N_A/V_M$ denotes the number of solvent lattice atoms per unit volume; V_M is the molar volume of the host metal lattice; and N_A(=6.0232x10^{23}atom/mol) is the Avogadro's number.

2.2 Elastic-Plastic Deformation in the Presence of Hydrogen

Elastic-plastic deformation can be easily modelled within ABAQUS using embedded constitutive equations. However, in the presence of hydrogen, the hydrogen-induced lattice deformation should be modelled through the dilatational distortion that accompanies the introduction of the hydrogen solutes into the lattice. To incorporate the hydrogen-induced lattice deformation, the deformation rate D_{ij} should be calculated from

$$D_{ij}=D_{ij}^{e}+D_{ij}^{p}+D_{ij}^{t} \tag{4}$$

with D_{ij}^{e}, D_{ij}^{p} and D_{ij}^{t} denote the elastic part, the plastic part and the part due to lattice straining by the solute hydrogen. The hydrogen-induced deformation rate D_{ij}^{t} is purely dilatational and is given by

$$D_{ij}^{t}=\frac{d}{dt}\left\{\ln\left[1+\frac{(C-C_o)\Delta\upsilon}{3\Omega}\right]\right\}\delta_{ij} \tag{5}$$

(express in tensor notation)

where C is total hydrogen concentration (in NILS and trapping sites) measured in hydrogen atoms per solvent atom; C_o is the initial hydrogen concentration in the absence of any straining; $\Delta\upsilon$ is the volume change per atom of hydrogen introduced into solution that is directly related to the partial molar volume of hydrogen $V_H=\Delta\upsilon\, N_A$ in solution; and Ω is the mean atomic volume of the host metal atom. The effective plastic strain ε_p should be calculated by

$$\varepsilon^{p}=\int\sqrt{\frac{2}{3}D_{ij}^{p}D_{ij}^{p}}\,dt \tag{6}$$

As the hydrogen-induced deformation rate, D_{ij}^{t}, is purely dilatational, it does not affect plastic strain and material hardening.

It is evident that the hydrogen diffusion is fully coupled with the stress analysis. For instance, Eq. (1) indicates that the calculation of the hydrogen distribution is coupled to the fields of the hydrostatic stress and effective strain. On the other hand, Eqs. (4)~(6) suggest that calculation of plastic strains requires determination of hydrogen concentration.

3. Finite Element Implementation to ABAQUS

To implement constitutive equations for hydrogen diffusion, given in Section 2, two user subroutines within ABAQUS are developed. The first one is UMATHT to define a material's thermal behaviour for the heat transfer analysis (in this paper hydrogen diffusion analysis), and the second one UMAT to define a material's mechanical behaviour to incorporate deformation rate induced due to lattice straining by the solute hydrogen. Detailed information on implementation is given below.

3.1 UMATHT

ABAQUS provides the built-in program for the heat transfer analysis[9]. An interesting point is that the governing equation for the heat transfer analysis is similar to that for transient hydrogen diffusion given in Eq. (1). The difference is variables involved in the governing equations. The UMATHT subroutine is used to match variables of the governing equations for heat transfer analysis with those for transient hydrogen diffusion. Table 1 summarizes equivalency of variables associated with two types of analyses. For instance, the specific heat in heat transfer analysis is equivalent to the effective diffusion constant in the hydrogen diffusion analysis.

To solve Eq. (1), however, information on plastic strains and on gradients of hydrostatic stresses is needed. This information is passed from the UMAT subroutine, which will be discussed in the next sub-section. Outputs from the UMATHT subroutine are the hydrogen concentration in NILS and trapping sites, C_L and C_T, respectively, which are passed into the UMAT subroutine to calculate the hydrogen-induced deformation rate using Eq. (5).

3.2 UMAT

Within the UMAT subroutine, the hydrogen-induced deformation rate is firstly calculated using Eq. (5) and the hydrogen concentration passed from the UMATH subroutine. It should be noted that the hydrogen-induced deformation rate depends on hydrogen concentration which should be calculated by solving the transient hydrogen diffusion equation, Eq. (1). Note also that, as the hydrogen-induced deformation rate is purely dilatational, it does not affect plastic strain and material hardening. Once the hydrogen-induced deformation rate is calculated, then the material's mechanical behaviour can be defined by implementing Eqs. (4)~(6) into the UMAT subroutine.

In addition, the gradient of the hydrostatic stress is also calculated within the UMAT subroutine. In the FE analysis, information on hydrostatic stresses is available at gauss points. To solve Eq. (1), however, it is preferred to calculate hydrostatic stresses at the nodal points rather than at gauss points. The reason is that calculation of the gradient using gauss point values could result in discontinuity between elements, which in turn could affect numerical stability. Thus, hydrostatic values at gauss points, passed from the ABAQUS main program, are extrapolated using the element shape function to determine hydrostatic values at nodal points, from which gradients can be calculated. The resulting gradients are passed into the UMATHT subroutines as an internal variable to solve Eq. (1).

Table 1 Analogy of variables between the heat transfer analysis within ABAQUS and the hydrogen diffusion analysis.

Heat transfer analysis (ABAQUS)		Hydrogen diffusion analysis	
Variable	Description	Variable	Description
$U(\theta)$	Thermal energy	$U(c)$	Chemical potential
T	Temperature	C_L	Interstitial hydrogen concentration
C_p	Specific heat	D_L/D_{eff}	Effective diffusion constant
ρ	Density	1	Unity
k	Conductivity	D_L	Diffusivity

3.3 Element Types

At present, the user subroutines are developed for the two-dimensional four-node quadrilateral element with full integrations. The four-node element with reduced integration has only one gauss point within the element, and thus has a problem in calculating the gradient of the hydrostatic stress, as calculated gradient values are discontinuous between elements. As two-dimensional eight-node elements with full or reduced integrations have sufficient gauss points, subroutines can be developed for eight-node elements. Eight-node elements, however, often exhibit fluctuating hydrostatic stress values and thus can cause numerical problems when hydrostatic stress gradients are calculated. It is believed that extension to three-dimensional elements is rather straightforward.

3.4 Flowchart

A flowchart for solving transient hydrogen diffusion within ABAQUS is shown in Fig. 1. As explained in previous sub-sections, the UMAT subroutine calculates plastic strains and gradients of the hydrostatic stress. Using these variables, the diffusion equation is solved in the UMATHT subroutine and thus the hydrogen concentration can be determined. However, it should be noted that calculation of plastic strains within the UMAT subroutine requires the hydrogen concentration according to Eq. (5). Thus calculations should be performed in an iterative manner. During iteration, the hydrogen concentration is updated, which affects not only plastic strains but also gradients of the hydrostatic stress. After several iterations (less than ten), the value of hydrogen concentration does not change (within the tolerance embedded in ABAQUS) and then the increment ends.

4. Comparisons with Published Results

4.1 Geometries, Materials and FE Meshes

To validate user subroutines implemented into ABAQUS for hydrogen diffusion simulations, simulated results are compared with published results in Ref. (4). Two types of test geometries were considered in Ref. (4). The first one was the boundary layer problem simulating small scale yielding under plane strain Mode I opening mode (see Fig. 2(a)). The second one was the plane strain (four-point) bend specimen with a round notch, as depicted in Fig. 2(b).

In simulations, low and high strength steels are considered in Ref. (4). Uni-axial stress-strain law of a material is assumed to be given by a power-law hardening relationship of the form

$$\varepsilon = \frac{\sigma}{E} + \left(\frac{\sigma}{\sigma_o}\right)^{1/N} \tag{7}$$

where σ_o is the yield strength, and E is the Young's modulus. For the low strength steel, the yield strength was set to σ_o=250MPa, whereas for the high strength steel, σ_o=1200MPa. The strain hardening exponent N was set to N=0.2 for both cases. For elastic properties, Young's modulus E=207GPa and Poisson's ratio ν=0.3 were used. Numerical data for simulations are taken from Ref. (4):

$$W_B = 60\text{kJ/mol} \;;\; N_A = 6.0232\times10^{23}\,\text{atom/mol} \;;\; N_L = 8.46\times10^{19}\,\text{atoms/mm}^3$$
$$V_H = 2.0\times10^{3}\,\text{mm}^3\text{/mol} \;;\; V_M = 7.116\times10^{3}\,\text{mm}^3\text{/mol} \;;\; D_L = 1.27\times10^{-2}\,\text{mm}^2\text{/s} \tag{8}$$

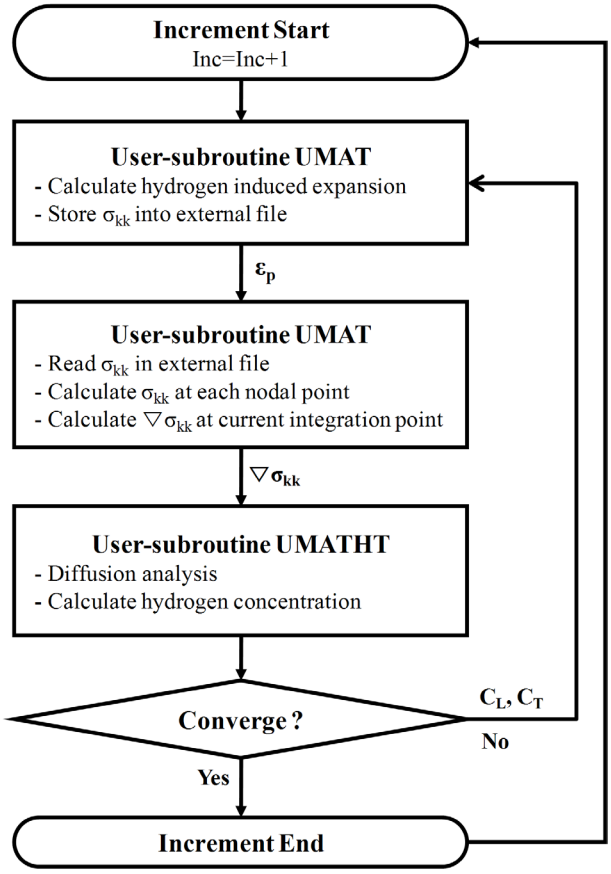

Fig. 1. A flow chart of simulation procedure.

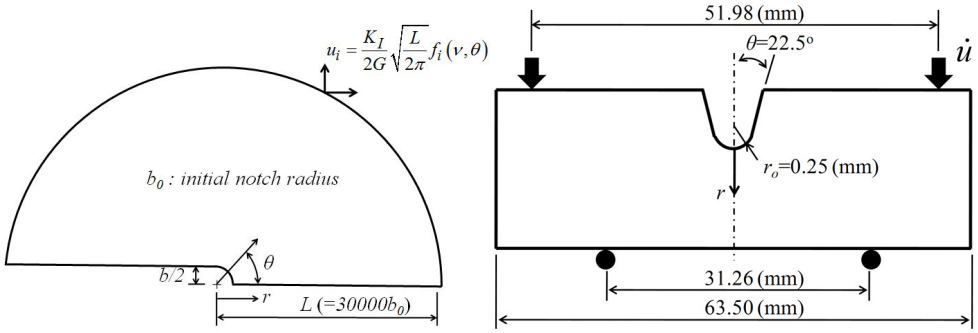

(a) (b)

Fig. 2. Two geometries considered in the present work to validate developed user subroutines: (a) the boundary layer approach simulating small scale yielding under plane strain Mode I opening mode, and (b) the plane strain (four-point) bend specimen with a round notch.

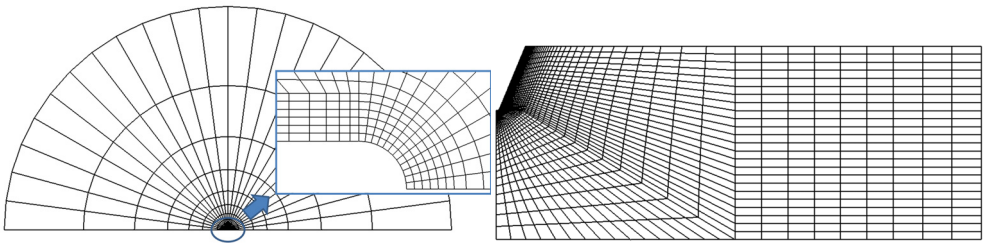

(a) (b)

Fig. 3. FE meshes: (a) the boundary layer problem and (b) the plane strain (four-point) bend specimen with a round notch.

Also the trap density N_T for iron and steels as a function of the local effective plastic strain ε_p is given by

$$\log(N_T) = 23.26 - 2.33\exp(-5.5\varepsilon_p) \tag{9}$$

The FE meshes for these two geometries are shown in Fig 3. Four-node plane strain elements for the coupled temperature-displacement analysis (CPE4T in ABAQUS) were used. For the boundary layer problem, the numbers of elements and nodes were 780 and 833, respectively. For the round-notch bend specimen problem, the numbers of elements and nodes were 1,816 and 1,906, respectively.

4.2 Boundary Conditions for Hydrogen Concentration

Regarding boundary conditions related to hydrogen concentration, two types are simulated. The first type is an "environmental embrittlement" condition by assuming that the specimen is under a uniform NILS hydrogen concentration, C_L=C_o at all times on the boundary of the specimen. The trapping site concentrations C_T follow from the NILS population through Eqs. (2) and (3). This boundary condition is referred to as the "constant concentration condition" in this paper. The second one is an "internal embrittlement". At time t=0, hydrogen is present both in NILS and in trapping sites, and two populations C_L=C_o and C_T are in equilibrium according to Eqs. (2) and (3). For t>0, all external surfaces including those of the crack or the notch are assumed to be insulated. This boundary condition is referred to as the "zero hydrogen flux" in this paper. For all

cases, the initial concentration C_o was set to 2.084×10^{21} hydrogen atoms/m^3.

4.3 Load Boundary Conditions

For the boundary layer problem, the load was applied as follows. Along the outermost boundary, the displacements were applied incrementally at a constant stress intensity factor rate up to a loading time $t=t_1$, at the end of which the final value of the Mode I stress intensity factor K_I was K_A. When $t>t_1$, the displacements were kept constant and hydrogen diffusion was allowed to continue. Values of K_A for the low strength and high strength materials were taken as K_A=89.7MPa√m and K_A=132MPa√m, respectively.

For the round-notched bend specimen, the loading was performed by prescribing constant displacement rate until loading was complete ($t=t_1$). The prescribed displacement rate was 0.002mm/s for the low strength steel. At times greater than t_1, the loading displacements were held constant and hydrogen diffusion continued under fixed held displacements.

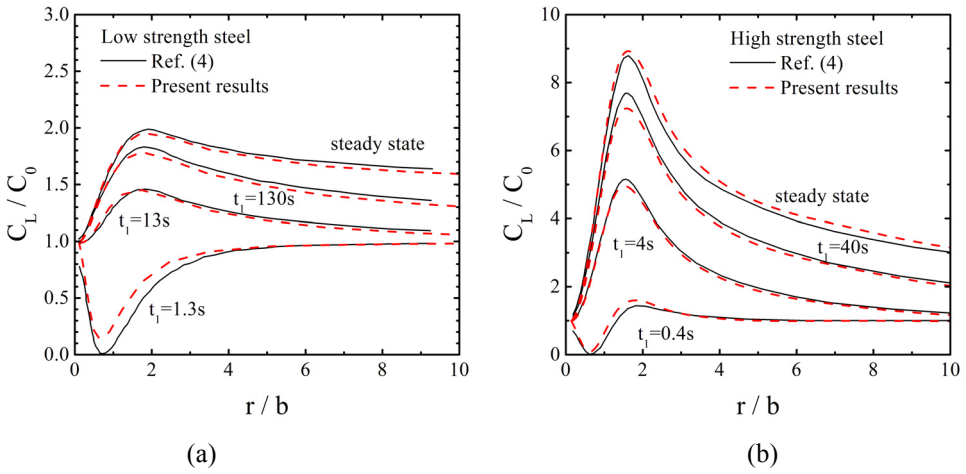

Fig. 4. Variations of the normalized concentration C_L/C_o in NILS with the normalized distance for the boundary layer problem with the constant concentration condition: (a) the low strength steel and (b) the high strength steel.

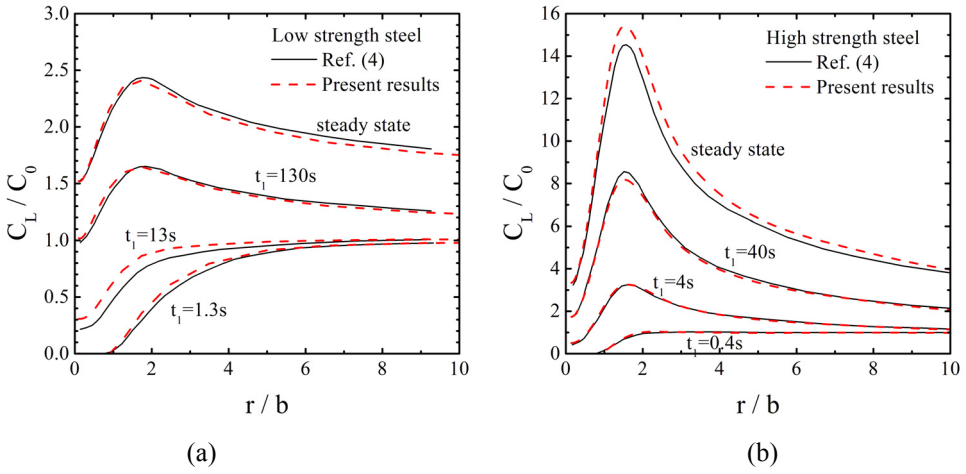

Fig. 5. Variations of the normalized concentration C_L/C_o in NILS with the normalized distance for the boundary layer problem with the zero hydrogen flux condition: (a) the low strength steel and (b) the high strength steel.

4.4 Results

Variations of the normalized concentration C_L/C_o in NILS with the normalized distance are shown in Fig. 4 for the boundary layer problem with the constant concentration condition. The distance r (from the notch root) is normalized with respect to the current crack opening displacement b (see Fig. 2(a) for the definition of r and b). In the figures, the results for $t=t_1$ indicate variations of C_L/C_o at time $t=t_1$, and the results for three different cases of t_1, t_1=1.3s, 13s, 130s, are shown. After sufficiently long times have elapsed, variations of C_L/C_o do not change with time anymore regardless of the choice of t_1, which are indicated as the steady state. Present FE results agree well with published ones in Ref. (4) for all cases considered. Corresponding results for the zero hydrogen flux are shown in Fig. 5, also showing good agreements with published results in Ref. (4).

Variations of the normalized concentration C_L/C_o in NILS and C_T/C_o in trapping sites for the notched bend specimen with the constant concentration condition are shown in Fig. 6. The distance r (from the notch root) is normalized with respect to the initial notch radius r_o (Fig. 2b). Corresponding results for the zero hydrogen flux are shown in Fig. 7. For all cases considered, present simulation results agree well with those in Ref. (4).

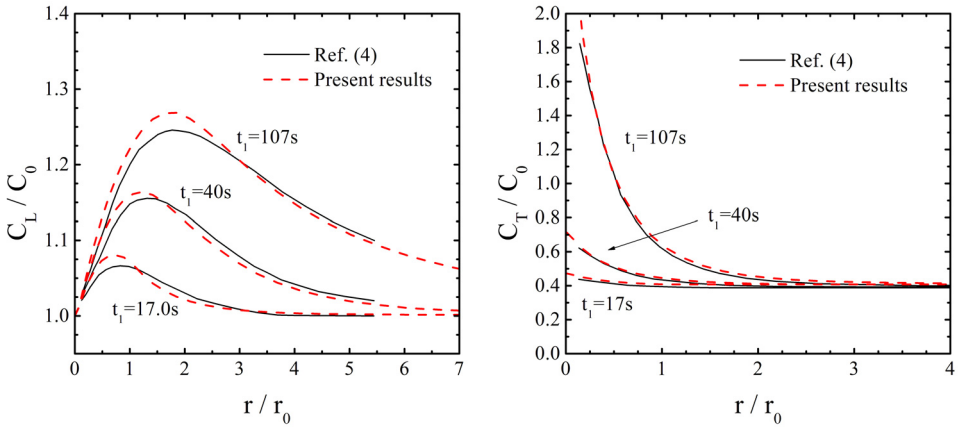

Fig. 6. Variations of the normalized concentration with the normalized distance for the round-notched bend specimen with the constant concentration condition: (a) C_L/C_o in NILS and (b) C_T/C_o in trapping sites.

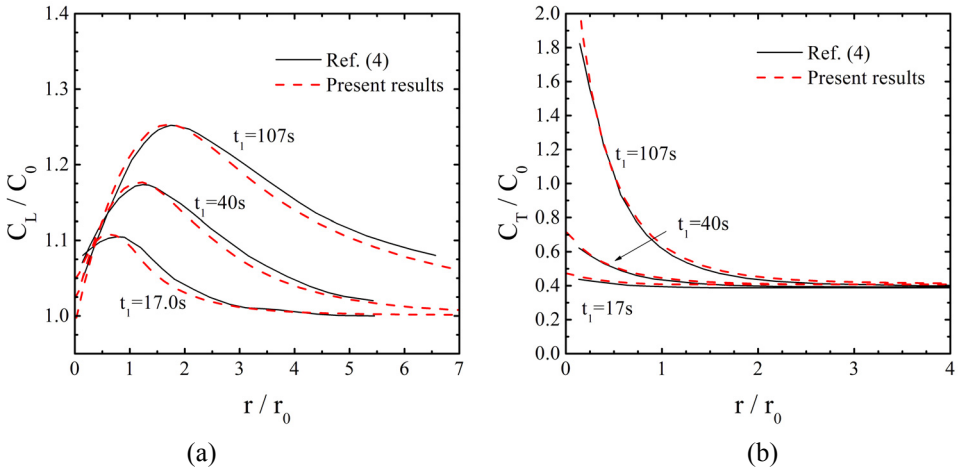

Fig. 7. Variations of the normalized concentration with the normalized distance for the round-notched bend specimen with the zero hydrogen flux condition: (a) C_L/C_o in NILS and (b) C_T/C_o in trapping sites.

5. Concluding Remarks

In this paper, a method to simulate coupled hydrogen transport equations using the general purpose FE program, ABAQUS is presented. Implementation focuses two key features in coupled hydrogen transport equations. One is to incorporate effects of the hydrostatic stress and plastic strain on hydrogen transport. To resolve this feature, the user subroutine UMATHT is developed. The other feature is to incorporate the hydrogen-induced dilatational deformation rate, which is resolved by the UMAT user subroutine. To validate developed user subroutines, present simulation results are compared with published ones in Ref. (4) for two types of geometries; the boundary layer problem and the plane strain bend specimen with a round notch. Comparisons show good agreements giving confidence in the use of developed subroutines for simulating coupled hydrogen transport equations using ABAQUS.

Acknowledgement

This work was supported by the MEST / KOSEF (Nuclear R&D Program, M2080608000208M060800210), the Korea Research Foundation Grant (KRF-2007-313-D00017) funded by the Korean Government. The author also wishes to acknowledge P-S Lam to motivate this work. During a recent conference, the authors found that a similar work was done independently[11]. Discussion with Mr. Falkenberg is appreciated.

References

(1)Hirth J.P., Effects of hydrogen on the properties of iron and steel, Metallurgical and Materials Transactions A, Vol. 11, No. 6 (1980), pp. 861-890.

(2)Birnbaum H.K. and Sofronis P., Hydrogen-enhanced localized plasticity-a mechanism for hydrogen related fracture, Material Science and Engineering A, Vol. 174 (1994), pp. 191-202.

(3)Sofronis P. and McMeeking R.M., Numerical analysis of hydrogen transport near a blunting crack tip, Journal of the Mechanics and Physics of Solids, Vol. 37, No. 3 (1989), pp. 317-350.

(4)Taha A. and Sofronis P., A micromechanics approach to the study of hydrogen transport and embrittlement, Engineering Fracture Mechanics, Vol. 68 (2001), pp. 803-837.

(5)Lufrano J., Sofronis P. and Birnbaum H.K., Modeling of hydrogen transport and elastically accommodated hydride formation near a crack tip, Journal of the Mechanics and Physics of Solids, Vol. 44 (1996), pp. 179-205.

(6)Lufrano J., Sofronis P. and Birnbaum H.K., Elastoplastically accommodated hydride formation and embrittlement, Journal of the Mechanics and Physics of Solids, Vol. 46 (1998), pp. 1497-1520.

(7)Liang Y., Sofronis P. and Aravas N., On the effect of hydrogen on plastic instabilities in metals, Acta Materialia, Vol. 51 (2003), pp. 2717-2730.

(8)Liang Y., Sofronis P. and Dodds RH Jr., Interaction of hydrogen with crack-tip plasticity: effects of constraint on void growth, Material Science and Engineering A, Vol. 366 (2004), pp. 397-411.

(9)ABAQUS Version 6.7. User's manual. Dassault Systemes, 2008.

(10)Oriani R.A., The diffusion and trapping of hydrogen in steel, Acta Metallurgica, Vol. 18 (1970), pp. 147-57.

(11)Falkenberg R., Simulation of crack growth due to a hydrogen-induced stress-corrosion cracking on a high-strength steel FeE690T, Proceedings of 17th European Conference on Fracture, (2008), Brno, Czech Republic.